Environmental Science
Nano

Accepted Manuscript

This article can be cited before page numbers have been issued, to do this please use: G. Metreveli, S. Kurtz, R. R. Rosenfeldt, F. Seitz, S. K. Kumahor, A. Grün, S. Klitzke, H. Vogel, M. Bundschuh, T. Baumann, R. Schulz, W. Manz, F. Lang and G. E. Schaumann, *Environ. Sci.: Nano*, 2021, DOI: 10.1039/D1EN00093D.

ROYAL SOCIETY OF CHEMISTRY

rsc.li/es-nano

View Article Online
DOI: 10.1039/D1EN00093D

Environmental significance

In order to enhance our knowledge on the distribution, transport, and impact of engineered nanoparticles in aquatic-terrestrial transition zones, the mesocosm studies simulating environmental conditions and scenarios are needed. The data obtained in this study indicate that the aggregation, sedimentation, and accumulation in/on biota represent major mechanisms controlling the fate of citrate-coated silver nanoparticles in such zones. However, a small fraction remaining in water for several weeks suggests long residence times and long-distance transport of nanoparticles in rivers. These efforts will boost the scientific understanding of the distribution and effects of nanoparticles in the environment especially over the long run and do provide a solid basis for the validation of nanoparticle fate or uptake models.

Distribution of engineered Ag nanoparticles in the aquatic-terrestrial transition zone: A long-term indoor floodplain mesocosm study

George Metreveli*[a], Sandra Kurtz[a], Ricki R. Rosenfeldt[b,c,d], Frank Seitz[b,c,d], Samuel K. Kumahor[e], Alexandra Grün[f], Sondra Klitzke[g,h,i], Hans-Jörg Vogel[e], Mirco Bundschuh[c,j], Thomas Baumann[k], Ralf Schulz[b], Werner Manz[f], Friederike Lang[h], Gabriele E. Schaumann[a]

[a] University of Koblenz-Landau, iES Landau, Institute for Environmental Sciences, Group of Environmental and Soil Chemistry, Landau, Germany

[b] University of Koblenz-Landau, iES Landau, Institute for Environmental Sciences, Group of Ecotoxicology and Environment, Landau, Germany

[c] University of Koblenz-Landau, iES Landau, Institute for Environmental Sciences, Group of Functional Aquatic Ecotoxicology, Landau, Germany

[d] nEcoTox GmbH, Annweiler, Germany

[e] Helmholtz Centre for Environmental Research - UFZ, Department of Soil System Science, Halle-Saale, Germany

[f] University of Koblenz-Landau, Institute of Integrated Natural Sciences, Department of Biology, Koblenz, Germany

[g] Berlin University of Technology, Institute of Ecology, Department of Soil Science, Berlin, Germany

[h] Albert-Ludwigs-Universität Freiburg, Institute of Forest Sciences, Chair of Soil Ecology, Freiburg, Germany

[i] German Environment Agency, Section II 3.1, Berlin, Germany

View Article Online
DOI: 10.1039/D1EN00093D

[j] Swedish University of Agricultural Sciences, Department of Aquatic Sciences and Assessment, Uppsala, Sweden

[k] Technical University of Munich, Chair of Hydrogeology, Munich, Germany

† Electronic supplementary information (ESI) available. See DOI:

Abstract

The fate of engineered nanoparticles in the aquatic-terrestrial transition zone is decisive for their effect in the environment. However, our knowledge on processes within this interface is rather low. Therefore, we used a floodplain stream mesocosm to enhance our understanding of the long-term distribution and biological effects of citrate-coated silver nanoparticles (Ag-NPs) in this ecosystem. Parallel to pulsed dosing of Ag-NPs, we observed fluctuating but successively increasing concentrations of aqueous Ag, 88-97% of which was categorized as particles. The remaining dissolved fraction was mainly complexed with natural organic matter (NOM). The major Ag fraction (50%) was associated with the uppermost sediment layer. The feeding activity of benthic amphipods was largely unaffected, which could be explained by the low Ag concentration and complexation of released Ag^+ with NOM. According to our hypothesis, only a small nanoparticle fraction (6%) moved to the terrestrial area due to aquatic aging and enrichment of Ag-NPs in sediments and biota. Nanoparticle infiltration in deeper sediment and soil layers was also limited. We expect that a small fraction of nanoparticles remaining in the water for several weeks can be transported over large distances in rivers. The Ag-NPs accumulated in top layer of sediment and soil may serve as a source of toxic Ag^+ ions or may be remobilized due to changing physico-chemical conditions. Furthermore, the high enrichment of Ag-NPs on algae (up to 250000-fold) and leaves (up to 11000-fold)

bears risk for organisms feeding on those resources and for the transfer of Ag within the food web.

1 Introduction

Engineered nanoparticles (ENPs) released into surface waters can undergo aging and transformation processes and interact with biotic and abiotic interfaces. Aquatic-terrestrial transition zones (known also as floodplain areas) influencing the transport and distribution of several contaminants[1] can also play an important role in the further transfer of ENPs from aquatic to the terrestrial compartments. There are numerous studies evaluating the distribution, transformation, transport, and effects of ENPs in aquatic and terrestrial model systems.[2,3] Most of these studies apply well controlled laboratory-scale batch systems, which are, however, hardly reflective of the complexity of natural systems[2,4,5] particularly relevant amongst others for floodplain areas. The mesocosm studies with much higher degree of complexity allow the evaluation of the environmental fate and effects of ENPs under more realistic conditions.[6,7] Mesocosms simulate natural systems such as wetlands, ponds, lakes, paddy fields, grassland terrestrial areas, or estuarine systems and thus bridge the gap between lab-based and field studies.[8] The importance of mesocosm studies for the evaluation of fate and effects of ENPs in the environment,[5,9–11] the regulatory risk assessment[11,12] as well as for the parameterization and validation of related models[9] is well known. The studies on dissolved chemicals indicate the applicability of mesocoms to those systems, too.[13] Previous floodplain mesocosm studies showing the movement of ENPs from the aquatic to the terrestrial compartment[14] and their accumulation in soil,[14] aquatic[15,16] and terrestrial[14] plants, as well as in fish and insects[14] underline the role of floodplain zones and flooding dynamics for the distribution of nanoparticles between aquatic and terrestrial areas as well as between

View Article Online
DOI: 10.1039/D1EN00093D

abiotic and biotic systems. Besides, the changing wetting and drying cycles of soils promote the release of soil particles,[17] which may increase the relevance of particle-associated ENP transport.

The time scale applied in mesocosm studies evaluating the environmental fate and impact of different ENPs is very diverse spanning from few hours,[18] days,[18,19] and weeks[20–24] to few months[4,15,25–36]. Only a hand full studies lasted for up to 9-18 months.[14,16,37–39] Since several processes such as transport of ENPs in soil and their enrichment in sediment layers require long time periods, such long-term studies are particularly valuable. Furthermore, mesocosm studies simulating lotic freshwater systems such as rivers do not assess the linkage to adjacent floodplain areas[25,26] and mesocosm studies simulating the floodplain areas only consider the material exchange with lentic freshwater systems[14–16,18,19,37,38]. In order to closely simulate environmental scenarios and to complement our knowledge on the fate and effects of ENPs in aquatic-terrestrial transition zone, a combination of both lotic and lentic areas in one mesocosm system, an application of natural surface water and natural floodplain soil, an intermittent change of flooding and drying events, as well as a realization of water infiltration in sediment and floodplain soil considering long time scales are necessary.

To enhance our knowledge on the transfer of ENPs across ecosystem boundaries over several months, we developed an indoor floodplain stream mesocosm system, combining a lotic freshwater system with a terrestrial compartment in one system. Since the silver is the most frequently used nanomaterial in consumer products,[40] we selected citrate-coated silver nanoparticles (Ag-NPs) as model ENPs. Aging, distribution, transport, accumulation, and effects of Ag-NPs in aquatic-terrestrial transition zone were assessed over several months using natural river water and

floodplain soil as matrixes under a regular flooding and drying scenario. In order to evaluate the ecotoxicological impact of Ag-NPs on the benthic organisms, we determined the *Gammarus fossarum* feeding rate, which is considered as a robust, sensitive and ecologically relevant variable[41]. We tested the following hypotheses: 1. aquatic aging, enrichment in sediments, and attachment to biofilms, algae, and leaf litter are the most important mechanisms limiting the transfer of Ag-NPs from lotic aquatic system to terrestrial compartment during flooding; 2. biological effects of Ag-NPs on amphipods in aquatic-terrestrial transition zone are controlled by the complexation of released ions and low level of aqueous exposure concentrations of nanoparticles induced by their aquatic aging.

2 Material and methods

2.1 Mesocosm setup and experiment

The indoor floodplain stream mesocosm system (Figure 1, A, B, Figure S1 ESI†) is made of polypropylene (PP; IKT Technology, Landau, Germany). The mesocosm system consisted of an aquatic zone (AZ, length: 3.0 m, width: 0.6 m, high: 0.45 m), a permanently flooded zone (PFZ, length: 1.0 m, width: 0.15 m, high: 0.15 m) incorporated into the aquatic zone, and a floodplain zone (FZ, length: 1.0 m, width: 0.6 m, high: 0.45 m). In the AZ, the system was equipped with a paddle wheel in order to generate the water flow. A gravel (SILIGRAN, 2.0 - 4.0 mm, Euroquarz GmbH, Dorsten, Germany) layer 1 and 3 cm thick served as drainage on the bottom of the AZ and PFZ, respectively. Quartz sand (F 34, Quarzwerke GmbH, Frechen, Germany, the characteristics see in Table S1 ESI†.) placed on top of gravels served as sediment. The height of the quartz sand layer in the AZ and PFZ was 4 and 12 cm, respectively. The release of ions from quartz sand was checked in separate washing tests (experimental details see in the ESI†, section 1.3). The quantity was,

however, negligible relative to the ion concentration in river water which was used as aqueous phase in mesocosm (Figure S2 ESI†).

A preliminary mixing test for which the AZ was filled up with deionized water (MINISTIL, P22 with electrical conductivity meter LKMA1.0, Orben Wasseraufbereitung, Wiesbaden, Germany; experimental details see in the ESI†, section 1.4 and Figure S3) indicated that 4 cycles of water movement in the AZ are needed to achieve a complete mixing (Figure S4 ESI†) between the tracer (salt) and the aqueous phase. Before the start of the actual experiment with Ag-NPs, the gravel and quartz sand were completely removed, the system was washed several times with deionized water to avoid any cross contamination with salt which may influence nanoparticle fate. Subsequently, the AZ and PFZ were refilled with fresh gravel and quartz sand as before. After filling, the gravel and quartz sand were washed with deionized water and the washing water was removed from the mesocosm.

The FZ, which was connected to the AZ via a perforated wall, was composed of a 5 cm drainage gravel layer covered by a 20 cm soil layer. The soil was collected from a floodplain area at the River Rhine (details see in the ESI†, section 1.5). Grain size distribution, total C, H, N, and S content, and pH of the soil (experimental details see in the ESI†, section 1.5) are summarized in the ESI†, Table S2. The soil was classified as clayey silt.[42] Additionally, the mesocosm system was equipped with two water percolation columns located in the FZ and PFZ, respectively. Both columns were filed up with gravel (5 cm drainage layer on the bottom) and soil (45 cm layer for the column in the FZ and 35 cm layer for the column in the PFZ).

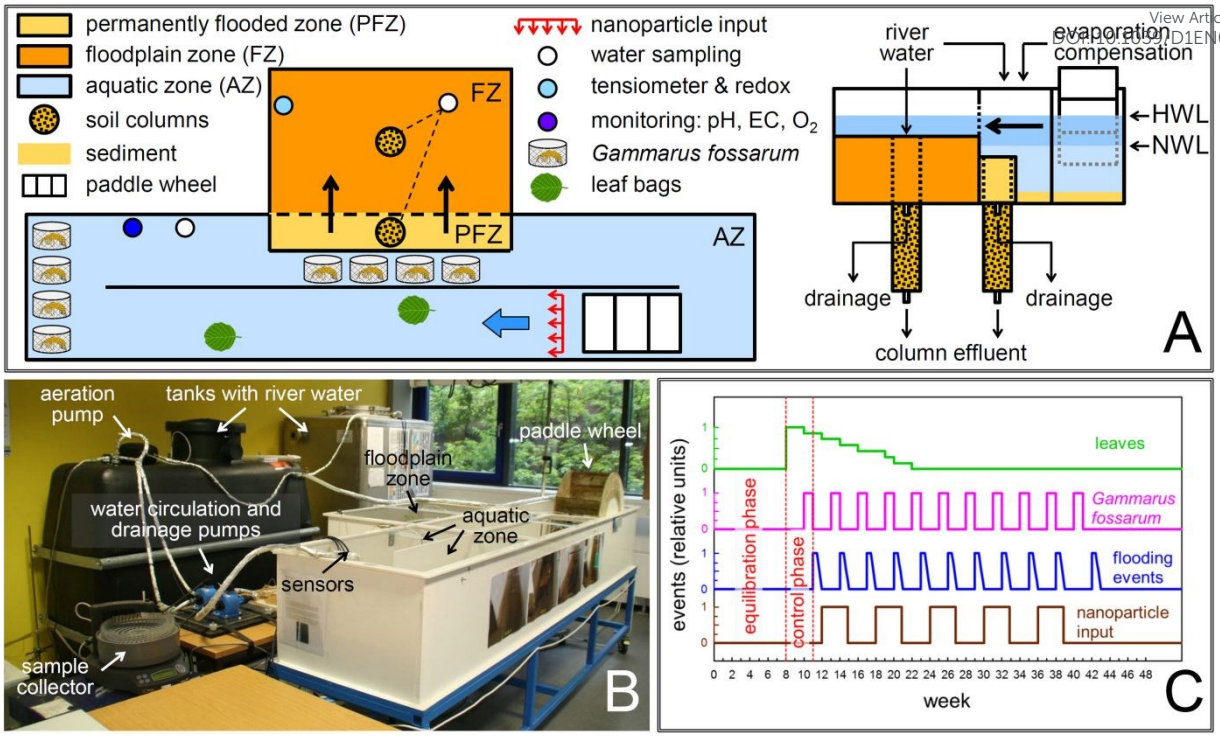

Figure 1. Experimental setup of the mesocosm system with top (left) and side (right) view (A). Photograph of the mesocosm system at the last phase of the experiment (B). Schematic representation of different events in mesocosm experiment (C). The abbreviations HWL and NWL in (A) refer to "high water level" and "normal water level", respectively, with HWL being achieved during flooding events. The values of "0" and "1" on the Y-axis in (C) show "no event" or the implementation of an event, respectively. The decreasing profile for leaves in (C) represents the relative amounts of leaves remaining in mesocosm after each sampling.

The AZ of the mesocosm was filled with 375 L natural river water collected from River Rhine (for sampling see ESI†, section 1.5 and for water quality parameters see ESI† Figure S5), which corresponded to a water level of 23 cm (normal water level). The paddle wheel induced a water flow of approx. 0.03 m s^{-1} in the AZ. In order to ensure stable bio-chemical conditions, the mesocosm was equilibrated for eight weeks. During this equilibration phase, river water circulated between AZ and water tanks,

View Article Online
DOI: 10.1039/D1EN00093D

with the latter serving as reservoirs, using submersible (Aquarius UP2, Oase, Hörstel, Germany) and oscillating piston (Typ V 12 mm, Wilhelm Keller GmbH, Nehren, Germany) pumps. Subsequently, a control phase of three weeks was realized during which the paddle wheel remained active, but AZ and water tanks were disconnected. In order to avoid the water stagnation in sediment (PFZ) and soil (FZ), water from the outlets of both zones was continuously removed at a flow rate of 1 cm d^{-1} (IPC ISM934 and MV-CA 8, Ismatec SA Laboratoriumstechnik, Glattbrugg-Zürich, Switzerland). To realize the infiltration, water was also continuously removed from the outlets of soil columns at a flow rate of 1 cm d^{-1}. After control phase, eleven flooding events followed by a period without flooding were simulated every three weeks with the duration of five days, respectively. To initiate flooding, equilibrated water was pumped from water tanks into the AZ to increase the water level from 23 to 27 cm (high water level). As a consequence, the FZ was also flooded (Figure S6, A, Figure S7, A ESI†). During floodings, the flow rate at the outlet of the FZ column was set at 20 cm d^{-1}. After five days, the water level was reduced to normal level (Figure S7, B ESI†) removing water from AZ. Subsequently, the outlet of the FZ was completely opened allowing water to drain the soil by gravity. After two days, the flow rate at the outlet of FZ was again adjusted at 1 cm d^{-1}. During experiment, the compensation of evaporation losses in mesocosm was done by periodical addition of deionized water into AZ.

After the first flooding event, a dispersion of citrate-coated Ag-NPs (5 mg L^{-1}) was continuously introduced (0.5 mL min^{-1}) into the AZ for three weeks. Ag-NPs were introduced into AZ by a capillary system (Figure S6, B ESI†). During the subsequent three weeks, no Ag-NPs were introduced. This rhythm was repeated five-fold through the study duration of 48 weeks. The repeatedly pulsed input of Ag-NPs is founded by

the lack of replication of indoor floodplain stream mesocosms and allowed for timely pseudo replicates in the same system. Ag-NPs were synthesized in house using a citrate reduction method with details being provided in our earlier studies[43,44] and in the ESI†, section 1.7. The initial Ag-NPs were characterized by dynamic light scattering (DLS), zeta potential measurements, transmission electron microscopy (TEM), and scanning electron microscope (SEM) (ESI†, section 1.7). The potential interaction between nanoparticles and polypropylene material of mesocosm was investigated in separate experiments (for experimental details see the ESI†, section 1.8).

In order to investigate the enrichment of Ag-NPs on leaves, 20 plastic mesh bags filled with black alder leaves were installed in the AZ (Figure S6, C ESI†). The ecotoxicological impact of Ag-NPs was determined every three weeks using the feeding rate of *Gammarus fossarum* (*G. fossarum*) as response variable. The field sampling location, acclimatization procedures, and selection criteria of gammarids as well as the information on the preparation of leaf discs are reported elsewhere.[45] The feeding was assessed in proximity to the sediment or in the middle of the water column for low flow (left edge of the AZ where the water flow turns) and high flow (between PFZ and center wall of the AZ) exposure scenarios (locations are indicated in Figure 1, A, see also the ESI†, Figure S6, D, E, Figure S7, C, red and yellow arrows) over one week each (n = 15). Therefore, one *G. fossarum* and two pre-weighted and pre-conditioned leaf discs (diameter: 2 cm) were set in a stainless steel cage (mesh size: 0.5 mm) and cages were kept in the AZ. The feeding assays were performed eleven times in total. The feeding rate of gammarids measured in a separate uncontaminated stainless steel channel filled with river water and located in the same room served as a control. In this channel, a paddle wheel generated the

View Article Online
DOI: 10.1039/D1EN00093D

water flow. The physico-chemical conditions (temperature, flow, and chemical composition of water) were similar to the mesocosm. Confidence interval testing was applied to assess for significant median differences in feeding over the whole experiment.[46] The different events and phases of the mesocosm experiment are schematically shown in Figure 1, C.

2.2 Collection of samples and monitoring of water chemical properties, soil humidity and redox potential

Water temperature, pH, oxygen concentration, and electrical conductivity were continuously measured in the AZ (SENECT aquatic technology, Landau, Germany, measurement location and sensors are shown in the ESI†, Figure S6, F). For further analysis, the water samples were collected in triplicates from the AZ three times per week and from the FZ once during each flooding event. The column effluents of 9-10 mL were continuously collected every 10 hours between floodings and every 5 hours during flooding events using an automatic fraction collector (Frac-920, Amersham Biosciences, Uppsala, Sweden). Furthermore, water samples from the 20-22 L drainage outlets of the FZ collected for last three flooding events were also selected for the analysis. The collected water samples were stored at 4°C until measurements.

In the water samples collected from the AZ, FZ, and soil column effluents, DOC (after filtration by 0.45 µm Teflon filter) and TOC concentrations were determined every week using a TOC analyzer (Multi N/C 2100S, Analytik Jena AG, Jena, Germany). The concentrations of anions (Cl^-, NO_3^-, SO_4^{2-}, F^-, PO_4^{3-}) and cations (Ca^{2+}, Mg^{2+}, K^+, Na^+) were quantified in AZ (every 8-10 weeks) and column effluent (every 4 weeks) water samples using ion chromatography (881 Compact IC pro, Metrohm AG, Herisau, Switzerland). The redox potential of FZ soil was measured at a depth of 5

and 15 cm (ecoTech, Bonn, Germany). Furthermore, the water potential of FZ soil was monitored at a depth of 5 cm (tensiometer, Keller, Winterthur, Switzerland).

Leaves from the deployed leaf bags were sampled at several time points after start of experiment to assess for potential Ag accumulation (Figure 1, C). During the experiment, an algae growth was observed resulting in a biofilm formation on the sediment, mesocosm walls, and paddle wheel although the organisms were not intentionally added to the mesocosm. In the FZ, plants, which were also not seeded, germinated and grew. After termination of the experiment, the water was removed from the mesocosm and biofilms, plants, sediment, and soil were sampled to determine Ag contents. The sediment and soil samples were collected from several locations and depths (Figure S8 ESI†). In order to determine the retention of Ag in the soil as a function of depth, the soil columns, removed from the PFZ and FZ were cut in layers (Table S3 ESI†). More details on the collection and pre-treatment of leaf, algae/biofilm, plant, sediment, and soil samples can be found in the ESI†, section 1.9. For the identification of Ag-NPs and their aggregates in biofilm, sediment, and soil samples, SEM measurements in combination with energy-dispersive X-ray spectroscopy (EDXS) were performed. Biofilm samples were additionally characterized in scanning transmission electron microscopy (STEM) mode. Experimental details on these methods are given in the ESI†, section 1.10.

2.3 Determination of Ag concentration and content in aqueous and solid samples

In order to find an optimal method for the determination of total Ag concentration in water samples, we tested several methods of sample storage, digestion, and analysis (details are given in the ESI†, sections 1.11-1.13 and Figure S9) and decided to store all aqueous mesocosm samples at 4°C and analyzed them without ultrasonic pre-

View Article Online
DOI: 10.1039/D1EN00093D

treatment by ICP-MS after microwave assisted acid digestion (the experimental details on the microwave digestion see in the ESI†, section 1.13).

To measure the dissolved Ag fraction released from Ag-NPs and to evaluate the possible formation of dissolved complexes between Ag^+ ions and natural organic matter (NOM), selected aqueous samples were filtered with 3 kDa and 50 kDa centrifugal ultrafiltration membranes (Amicon Ultra-15 centrifugal filter device, Merck, Millipore) at 2576 g for 60 min. The filtrates (10 mL) were acidified with 150 µL HNO_3 (65%, sub-boiled) and measured by ICP-MS.

The quantification of Ag in leaf, plant, and algae/biofilm samples required a digestion by HNO_3 in a water bath set at 80, 80, and 60°C, respectively. After digestion, the content of Ag was measured by ICP-MS. For biofilm and leaves, we also determined the Ag enrichment factor which relates the Ag content of dry biofilm or leaf to the Ag exposure concentration in the water phase. The total Ag content of sediment and soil samples was measured by ICP-OES after microwave assisted digested in a diluted mixture of HCl and HNO_3 (HCl/HNO_3 volume ratio: 2.5/1). The details on the digestion methods and quality control are given in the ESI†, section 1.14 and Figure S10.

A mass balance of Ag was based on the data obtained from all matrices determined. The fractions of Ag were calculated from measured mean Ag concentration in input dispersions (4843 µg L^{-1}). In the mass balance, the fraction of Ag removed from mesocosm system by removing water after the flooding events (approx. 160 L per flooding event) and through sampling was considered.

3 Results and discussion

3.1 Properties of initial Ag-NPs and physico-chemical conditions in mesocosm

The particle size distribution of citrate-coated Ag-NPs in stock dispersion was unimodal (Figure S11 ESI†) with z-average hydrodynamic diameter of 35.0 ± 0.5 nm and polydispersity index of 0.35 ± 0.01 measured directly after synthesis (mean ± SD, n = 6, Figure S12, A ESI†). As observed by TEM and SEM measurements, the Ag-NPs represented a mixture of quasi-spherical and rod-like particles (Figure S12, C-F ESI†). Similar to observations in our earlier study,[43] the share of rod-like particles was about 20%. The Ag-NP dispersions showed high colloidal stability for 5 years (Figure S12, A ESI†) which can be explained by their high negative zeta potential of -55.3 ± 3.2 mV (mean ± SD, n = 15, Figure S12, B ESI†) and consequently by strong electrostatic repulsion. The high colloidal stability supported our plan to use one source of Ag-NPs for all five periods with nanoparticle input in the mesocosms.

Since the mesocosm room was not air-conditioned, the water temperature varied between 17°C and 23°C (Figure S13 ESI†). The oxygen saturation of water was between 80% and 100% corresponding to oxygen concentrations of 7.5-9.5 mg L^{-1} supported by continuous aeration of the water tanks and water movement induced by the paddle wheel. The pH of the water was between 7.9 and 8.6 deviating little form the value determined in the river water directly after sampling (pH = 7.9). This indicates that the system was in a thermodynamic equilibrium regarding the concentration of protons during whole experiment. Electrical conductivity varied between 320 and 470 µS cm^{-1} reaching the maximum at week 28, which coincided with a simultaneous increase in concentration of ions especially Ca^{2+} and NO_3^- (Figure S14, A, B ESI†). This increase is most likely due to the release of ions from the soil matrix of the FZ and both soil columns. A presence of bicarbonate anions is

also expected but the applied method of ion chromatography did not allow their determination. The fluctuation of electrical conductivity over time is related to evaporation and compensation of such losses by the amendment of deionized water as well as the initiation of flooding events. The DOC and TOC concentrations varied between 2 and 6 mg L^{-1} with slightly higher concentrations between week 8 and 20 (Figure S15, A ESI†). This fluctuation in OC levels may be a consequence of algae growth observed already during the control phase as well as the release of OC from the leaves added to the mesocosm between equilibration and control phases. Furthermore, washout of OC from the soil of the FZ and both columns cannot be excluded. Further development in ion and OC concentrations was most likely controlled by limited availability of easily mobilized ions and OC at the late stages of the experiment.

With water infiltration into PFZ and FZ soil columns, Ca^{2+}, Mg^{2+}, NO_3^-, and partly Na^+ (PFZ column) ions were washed out while their enhanced concentrations in column effluents decreased slightly with time (Figure S14, C-F ESI†). In contrast to this, the concentrations of K^+, Cl^-, and partly Na^+ (FZ column) remained constant and in the same range as in the water phase of AZ. The DOC and TOC concentrations in the column effluents (Figure S15, B ESI†) were much higher than in the water phase of the AZ and FZ and showed leaching profiles typical for soils rich in OC[47]. The OC concentrations in the column effluents decreased from 115 mg L^{-1} to 24 mg L^{-1} and from 86 mg L^{-1} to 20 mg L^{-1} for PFZ and FZ column, respectively. The higher mobilization from the column in the PFZ may be related to its permanent and complete water saturation, while the column in the FZ was only saturated during flooding but sprinkled with water on the column surface between flooding events.

View Article Online
DOI: 10.1039/D1EN00093D

The redox potential in FZ soil was positive at a depth of 5 cm and thus higher compared to the redox potentials determined at 15 cm depth which were predominantly negative (Figure S16, A ESI†). This may be explained by higher oxygen availability in the top layers of soil. Furthermore, the redox potential was affected by flooding events. At the depth of 5 cm, the redox potential decreased during flooding indicating a reduced diffusion of oxygen through the overlying water. In contrast to this, the redox potential sometimes increased during flooding at 15 cm depth most likely due to the availability of fresh water from AZ transporting more oxygen to the deeper soil layers. The tensiometer pressure determined in the soil of the FZ showed high water saturation during and decreasing saturation in-between flooding events (Figure S16, B ESI†).

3.2 Ag in the water phase

In the water samples collected from the AZ and FZ, total Ag concentration fluctuated but successively increased (Figure 2). The total Ag concentrations varied between 5 and 37 µg L^{-1} with peaks coinciding with the periodic Ag-NP input. The decrease in total Ag concentrations between Ag-NP input pules can be explained by aquatic aging of nanoparticles. We suggest that the aggregation and sedimentation are the most important processes occurring after introduction of nanoparticles into the water phase of mesocosm. In our earlier study, we systematically investigated the homo-aggregation dynamics of similar citrate-coated Ag-NPs dispersed in synthetic and natural Rhine water, chemically similar to the Rhine water applied in mesocosm experiment and determined the critical coagulation concentration (CCC) of Ca^{2+} in Rhine water at 1.49 ± 0.03 mmol L^{-1}.[43] Since the concentration of Ca^{2+} in the mesocosm water of present study varied between 1.24 ± 0.04 and 1.44 ± 0.04 mmol L^{-1} (Figure S14, A ESI†), we can assume the homo-aggregation of

Ag-NPs under a reaction-limited regime as well as close to the CCC under a diffusion-limited regime. This suggests a formation of both compact reaction-limited and loose and fractal diffusion-limited homo-aggregates[48] in the present study.

The results of the present study are well in line with other studies. These studies reported the homo-aggregation for gum arabic (GA)-coated Ag-NPs and Ag_2S-NPs[16] as well as for polyvinylpyrrolidone (PVP)-coated Ag-NPs[14] in freshwater wetland outdoor mesocosms run with groundwater. In contrast to this, no evidence for the homo-aggregation of the PVP-coated[31,32] and citrate-coated[32] Ag-NPs was observed in littoral lake outdoor mesocosms. The deviation in results may be explained by the much lower ionic strength and higher DOC concentration compared to our study. However, the formation of hetero-aggregates was not excluded by these authors explaining the increased Ag concentration in the particulate fraction (0.2-35 µm).[32] In surface waters, the formation of hetero-aggregates with natural particles is in fact expected to be the major aggregation mechanism if the nanoparticle concentrations are low.[49] Consequently, hetero-aggregation may also be a relevant process in our study.

The adsorption of Ag-NPs to the PP material of the mesocosm may contribute to the reduction in total Ag concentrations. However, sorption tests revealed that the total Ag concentration in batch setting dropped from 100 µg L^{-1} to 7-27 µg L^{-1} independent of the presence of PP (Figure S17 ESI†). This decrease in the Ag concentration may hence be mainly explained by Ag-NP aggregation and sedimentation and not by their adsorption onto PP. In addition to this mechanism, Ag accumulation on algae and leaves has been important process influencing Ag distribution and is discussed below.

View Article Online
DOI: 10.1039/D1EN00093D

Despite these mechanisms, some Ag remained dispersed in the water for several weeks. At the end of the experiment (8 weeks after last nanoparticle input), for example, 5 µg L^{-1} total Ag was determined suggesting a potential for long-distance transport in rivers and streams. This idea is supported by a recent finding highlighting the transport of anthropogenic Ag-containing nanoparticles in one river approximately 150 km downstream of the discharge point, a wastewater treatment plant effluent.[50]

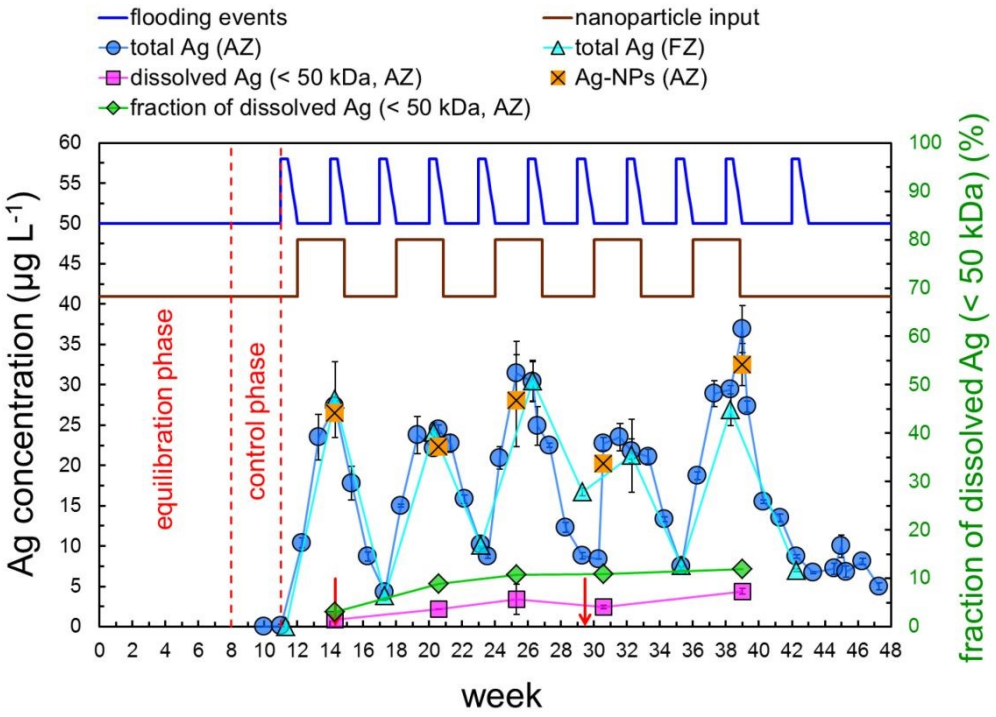

Figure 2. Mean ± SD (standard deviation) water concentrations (n = 3) of total, dissolved (< 50 kDa), and particulate Ag and fraction of dissolved Ag (< 50 kDa) over the duration of the experiment. The vertical red arrows show the sampling times of water samples filtered with 3 kDa membrane for which the Ag concentration in filtrate was below the limit of quantification of detection method.

Since the initial Ag-NP dispersion does not contain particles smaller than 6 nm,[43] we can assume that the Ag determined in the filtrate of 50 kDa membrane corresponding to a pore size of approximately 5 nm,[51,52] represents only dissolved Ag. The filtrate concentration of Ag-NPs passing the membrane as a consequence of particle size reduction due to the dissolution is negligible since the mass weighted fraction of small (6-12 nm) particles was only 0.07%[43]. The concentration of dissolved Ag increased from 1 µg L^{-1} to 4 µg L^{-1} between weeks 14 and 39 corresponding to 3-12% of the total concentrations of aqueous Ag (Figure 2). The main part of Ag (97-88%) was available as particles. The Ag concentrations measured in the filtrates of 3 kDa membrane, which was applied for selected water samples, were below the limit of quantification (LOQ) of ICP-MS (0.2 µg L^{-1}). Our earlier work showed that the 92 ± 8% and 90 ± 12% of Ag^+ ions pass the 3 kDa and 50 kDa membranes, respectively.[53] Consequently, we can assume that the dissolved Ag released from Ag-NPs was most likely complexed by NOM molecules with molecular weights between 3 and 50 kDa. This assumption is supported by the observations describing the formation of dissolved complexes between Ag^+ ions and several types of NOM, such as Pony Lake fulvic acid (PLFA) reported in our earlier studies[53,54] or Suwannee River humic acid reported by other researchers[55]. Due to the low concentrations of dissolved Ag, we do not expect a formation of secondary Ag-NPs as a consequence of silver ion reduction by NOM. Such processes usually require concentrations of dissolved Ag several orders of magnitude higher than determined in our study.[56,57]

3.3 Ag in sediment and soil

The top sediment layer in the AZ and PFZ was enriched by Ag. In both zones, the uppermost 0.5 cm of the sediment showed an Ag content of approx. 11 µg g^{-1} (Figure 3, A and B). At lower layers (0.5-4.0 cm in AZ, 0.5-1.0 cm and 1.0-3.0 cm in PFZ), the

Ag content decreased significantly varying between 0.2 and 0.6 µg g^{-1}. In deeper layers of the PFZ, the Ag content was below the LOQ of the ICP-OES method (approx. 0.08 µg g^{-1}) and probably in the range of the natural Ag background levels of the sediment which could only be determined by ICP-MS (horizontal red lines in Figure 3, A and B). The strongly decreasing Ag contents with increasing depth suggest only weak transport of Ag-NPs in deeper sediment layers.

The high Ag content in the top sediment layer is most likely the consequence of the nanoparticle aggregation and sedimentation, which is assumed as a major mechanism triggering nanoparticles fate. Aggregates of Ag-NPs were observed on the sediment top layer by SEM and EDXS with a size between 550 and 770 nm (Figure 4, A-F). Despite suggested aggregation and sedimentation mechanism, we cannot exclude the attachment of nanoparticles onto the sediment grains due to the reduction of electrostatic repulsion forces as a consequence of charge neutralization by cations. An accumulation of nanoparticles in biofilm grown on the sediment surface can also limit their transport to deeper layers. Similar to our study, an enrichment of Ag was observed in the sediment top layer in littoral lake outdoor mesocosms.[32] As EDXS indicated higher levels of sulfur in sediments with Ag-NPs (Figure 4, B) compared to the area free of nanoparticles (Figure 4, C), partial sulfidation of citrate-coated Ag-NPs in our mesocosm is also possible. This observation is in line with other publications using PVP-coated[14] and GA-coated[16,37] Ag-NPs in outdoor freshwater wetland mesocosms. The accumulation of Ag-NPs on the sediment surface may make them a continuous source of Ag^+ ions leading to increasing risk for organisms over time. Furthermore, this immobilized Ag-NPs may be remobilized if physico-chemical conditions in river systems change as shown in a system simulating riverbank filtration.[58]

View Article Online
DOI: 10.1039/D1EN00093D

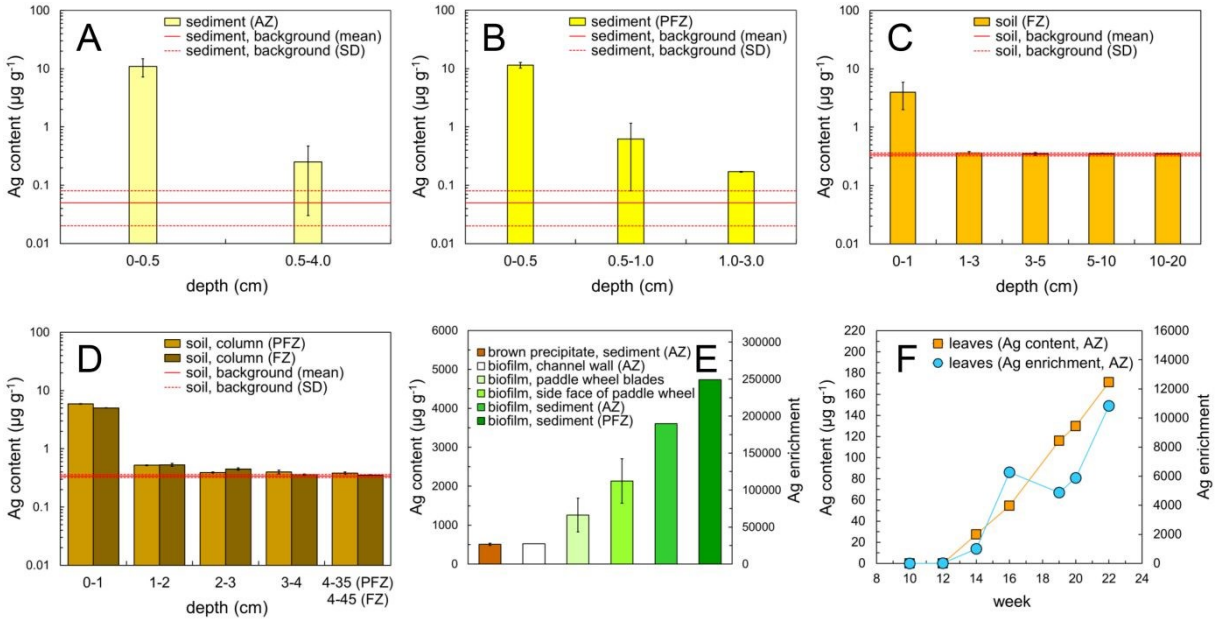

Figure 3. Mean ± SD Ag content (n = 3) in different depths of AZ (A) and PFZ (B) sediment, FZ soil (C), and PFZ and FZ soil columns (D). The Ag contents in the soil column layers from 4 to 35 cm (PFZ) and from 4 to 45 cm (FZ) depths were pooled. The natural background content of Ag in sediment and soil was not subtracted from the measured values but is indicated by red solid (mean value) and dashed (standard deviation) lines. The Ag content and enrichment in biofilm samples (E), brown precipitate (E), and leaves (F) normalized to their respective dry weight. The columns and error bars for biofilm samples collected on blades and side faces of paddle wheel and for brown precipitate (E) correspond to mean values and standard deviations (n = 4-10). The natural Ag background was subtracted from Ag content of leaves.

The Ag content in the soil top layer (0-1 cm) of the FZ was 4.0 ± 2.0 µg g^{-1} (Figure 3, C), which is lower compared to the Ag contents in the uppermost sediment layer. This observation is in line with our hypothesis 1 suggesting that aquatic aging and enrichment in sediments are the dominant mechanisms limiting the transfer of Ag-

NPs from aquatic to terrestrial compartment. As a consequence of the low Ag contents, SEM and EDXS could not confirm the presence of Ag-NPs on the soil surface. In contrast to the AZ and PFZ sediments, Ag-NPs were not retained in deeper soil layers. The Ag levels in these soil layers were at the natural background content of approx. 0.35 μg g^{-1} (Figure 3, C). No Ag was also determined in the effluents of FZ after flooding events despite the formation of cracks on the soil surface (Figure S18, F ESI†) as a consequence of drying between floodings. The data show that Ag is transported to the FZ but is not infiltrating the soil over the study duration set here.

In the soil columns located at the PFZ and FZ, Ag levels in the top layer (0-1 cm) reached 5.9 ± 0.1 μg g^{-1} and 5.0 ± 0.1 μg g^{-1}, respectively (Figure 3, D). The Ag content at 1-2 cm and 2-3 cm depth was one order of magnitude lower and varied between 0.39 and 0.53 μg g^{-1}. Deeper layers had Ag levels in the range of natural background (red line in Figure 3, D). Furthermore, no Ag was determined in the effluents of both columns during the entire experiment as concentrations were below the LOQ of ICP-MS. Considering the lengths of the soil columns and water flow rates, the time needed for the breakthrough of the water and particles which are not interacting with the soil material corresponds to 5.7 weeks for PFZ column and 0.4 weeks for FZ column but Ag-NPs remained only in the first 3 cm during the whole experiment. Consequently, the transport of Ag-NPs in soil columns was extremely slow compared to the water transport. This may be explained by low Ag concentrations in the overlying water as well as by the attachment of nanoparticles and their aggregates onto the soil grains due to the reduction of electrostatic repulsion forces as a consequence of charge neutralization especially by divalent

cations showing enhanced concentrations in the column eluates (Figure S14, C, E ESI†).

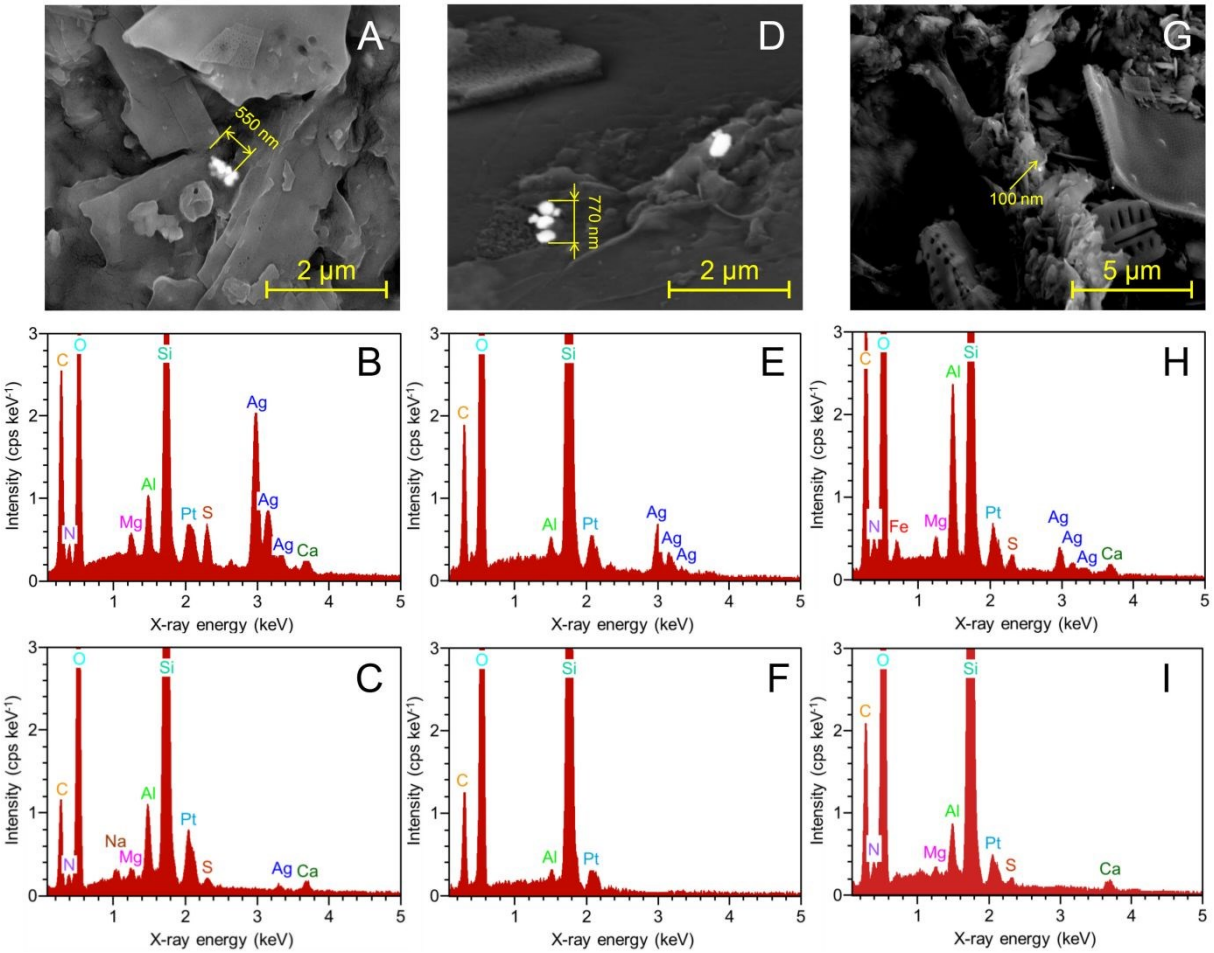

Figure 4. SEM pictures (A, D, G) and EDX spectra (B, C, E, F, H, I) of sediment samples from the AZ (A-C) and PFZ (D-F) and biofilm sample from the paddle wheel surface (G-I). All samples were collected after termination of experiment. The EDX spectra were measured for the areas in presence (B, E, H) and absence (C, F, I) of nanoparticles. Si peaks of the biofilm sample (H, I) are partly originated from silicon wafer used as sample carrier. Pt peaks are originated from Pt coating of samples. Due to the low Ag content, no nanoparticles were found in soil samples.

3.4 Ag enrichment in/on algae, leaves, and plants

During the mesocosm experiment, a biofilm growth was observed on various surfaces, that are the mesocosm walls, sediment (Figure S18, A, B ESI†), and paddle wheel (Figure S18, C, D ESI†). Algae colonizing the paddle wheel contained green algae (*Stigeoclonium* spec.) and diatoms (*Navicula* spec.) at the end of the experiment. The STEM (Figure S19 ESI†) and SEM (Figure 4, G) measurements confirmed the presence of diatoms. Biofilms on the sediment were composed of nematodes, cyanobacteria (*Pseudanabaena catenata*), diatoms (*Navicula* spec.), and rotifers. Most probably, increasing concentration of nitrate in our mesocosm water supported the biofilm growth. In contrast to nitrate, the concentrations of phosphate were below the limit of detection (LOD) of the applied method. However, due to the high LOD value (0.05 mmol L^{-1} or 4.5 mg L^{-1}) we cannot exclude the presence of phosphate at the concentrations higher than approx. 100 µg L^{-1} needed for biofilm growth[59]. Moreover, Ag showed a high affinity for biofilm. The SEM and EDXS analyses of these samples showed the presence of Ag-NPs (Figure 4, G, H, I) with a size of approx. 100 nm. For these samples, the signal of sulfur was also determined indicating nanoparticle sulfidation.

The biofilm Ag content and its enrichment factor, which relates the concentration in the biofilm to the exposure concentration in the water phase, were unexpectedly high. The Ag content and enrichment factor in biofilm collected from the mesocosm walls were 518 µg g^{-1} dry weight and 27000, respectively. Similar Ag content (506 ± 27 µg g^{-1} dry weight) was determined in a brown precipitate collected on the sediment surface (Figure S18, E ESI†) most probably representing the mixture of inactive algae, degradation rests of leaves, and feces of amphipods. Biofilms on the paddle wheel contained 1256-2133 µg Ag g^{-1} dry weight translating to an enrichment

factor in the range of 66000-110000 (Figure 3, E). The sediment biofilms had even higher Ag contents (3607-4732 μg g^{-1} dry weight) and enrichment factors (190000-250000). Those values are higher than those reported elsewhere for periphyton of oligotrophic lake mesocosms after chronic dosing of PVP-coated Ag-NPs.[32] However, these differences should be interpreted carefully due to the much lower concentration of major ions (Ca^{2+}, Mg^{2+}, Na^{+}, K^{+}, Cl^{-}, and SO_4^{2-}) and higher DOC concentration of this lake water compared to the present study as well as differences in the exposure scenario and type of nanoparticles. Although the presence of anionic nutrients such as nitrate and phosphate in this lake water were not reported, we can assume that the concentration of these anions were also lower than in our study. Furthermore, Ag-NPs can influence the biofilm growth depending on the nutrient concentrations[60] suggesting also different conditions for this oligotrophic lake and our mesocosm. Besides Ag enrichment, the information on the uptake mechanisms of Ag in biofilms is also important for the risk assessment. However, the determination of total Ag does not provide the information on the location of Ag in biofilms. From SEM and EDXS measurements we can assume that the nanoparticles are most probable attached to the surface of algae (Figure 4, G, H). This idea is supported by an earlier laboratory study suggesting that citrate-coated Ag-NPs are adsorbed onto algal surfaces or are bound to the extracellular proteins but they do not penetrate the cell wall and are hence not taken up.[61] The high Ag enrichment in biofilms observed in our study was most likely a result of the interplay between aggregation and sedimentation of Ag-NPs and their high affinity to algae and extracellular proteins.

Leaves submerged in the water of the AZ showed also an accumulation of Ag well exceeding its background level of 0.33 μg g^{-1}. Ag accumulated over time on the leaves and reached approx. 170 μg g^{-1} after 22 weeks, which translates to an

enrichment factor of approx. 11000 (Figure 3, F). High Ag content of leaves is most likely a result of high affinity of Ag for biofilms covering and decomposing leaves submerged in water[62]. Measurements could not be continued after week 22 as leaves degraded nearly completely and adding new samples would have undermined the goals of the study. Therefore, a direct comparison to Ag accumulation in biofilms grown on the sediment and paddle wheel surface is not possible. It is, however, obvious that the Ag content on the leaves was in the same order of magnitude as those detected in biofilms grown at the mesocosms wall at the termination of the experiment.

Furthermore, plants (Urticaceae and fern) grew in the soil of the FZ (Figure S18, F ESI†). Their Ag content ranged from 23 to 34 µg g^{-1} dry weight. The Ag accumulation by terrestrial plants grown in mesocosms was also reported for PVP-coated Ag-NPs.[14] Although the mechanisms explaining the enrichment of Ag in the biological substrates have not been experimentally clarified in the present study, the rather higher Ag contents suggest an enhanced risk for the organisms feeding on those resources with a possibility for Ag transfer within aquatic and terrestrial food webs.[63]

3.5 Mass balance

Ag was distributed among all compartments covered in the present mesocosm experiment with the amount of Ag retained being highly variable among those compartments (Figure 5). The largest fraction (52.4 ± 21.1%) of total Ag was present in the sediment of the AZ. The sediment of the PFZ retained only 3.3 ± 0.4% Ag. This difference can be explained by the approx. 15-fold lower sediment mass of the PFZ considered in calculations compared to the AZ. The major part (approx. 50% of total Ag introduced into the mesocosm) of Ag in sediments was in turn associated with their respective top layer. Similar to this, the littoral lake mesocosm study reported

View Article Online
DOI: 10.1039/D1EN00093D

also higher recoveries for PVP- and citrate-coated Ag-NPs in the top sediment layer compared to the deeper layers[32] but the recovery values were 2-4-fold lower than in sediment of our mesocosm due to the much lower ionic strength and higher DOC concentration compared to our study. The amount of Ag retained in the soil of the FZ and in the soil columns was 6.0 ± 3.1% and 0.14 ± 0.01%, respectively. This indicates that relatively low but not negligible amount of Ag can be moved to the terrestrial compartment by floodings. However, the transport in the deeper soil layers is strongly limited. The share of Ag in the biological compartments was lower compared to the sediment and soil. The Ag fraction found in/on plants, leaves, brown precipitate, and biofilms was 0.03%, 0.27%, 0.28 ± 0.02%, and 1.2 ± 0.8%, respectively, adding up to approx. 2% of the total Ag at the termination of the experiment. The fraction of Ag remaining in the water phase was also low (0.77 ± 0.04%). However, this fraction of Ag was determined in the water phase 8 weeks after last nanoparticle input suggesting long residence times and long-distance transport of nanoparticles in rivers.

The recovery rate of the total introduced Ag was 64.5% with a standard deviation of 25.5%. This high variability is a result of the highly heterogeneous distribution of Ag especially in sediments within the AZ. Consequently, the Ag recovering in the whole system ranged from approx. 39 to 90%. This high fluctuation is in line with another study evaluating the transport of Ag-NPs in an outdoor riverbank filtration system with Ag recoveries ranging from 54 ± 24% to 132 ± 25%.[58] An increase in the number of sampling locations would obviously reduce this uncertainty but requires higher resources. We need to admit that we have not quantified the possible losses of nanoparticles on the stainless steel cages and plastic mesh bags used for

amphipods and leaves, respectively. Although such losses are considered as low, this point could partly contribute to the non-recovered Ag mass.

In our mesocosm, citrate-coated Ag-NPs selected as model nanoparticles showed partly similar behavior as GA-[16,37] and PVP-coated[14,32] Ag-NPs as well as Ag_2S-NPs[16] in other mesocosm studies. This can be explained by similar aging processes. However, the low number of the mesocosm studies evaluating the fate and effects of Ag-based nanoparticles and the differences in physico-chemical conditions as well as in exposure scenarios do not allow to suggest one type of Ag-NPs as representative of other Ag-NPs.

The mass balance shows that the results of the mesocosm experiment confirm our hypothesis 1 suggesting the aquatic aging, enrichment in sediments, and accumulation in/on biota as major mechanisms limiting the transfer of Ag-NPs from aquatic to terrestrial compartment. Information on the mass balance for nanoparticles is essential for the correct interpretation and understanding their environmental fate and effects. However, up to now, only few studies presented and discussed the mass balance for Ag-NPs introduced into mesocosm systems.[14,16,32]

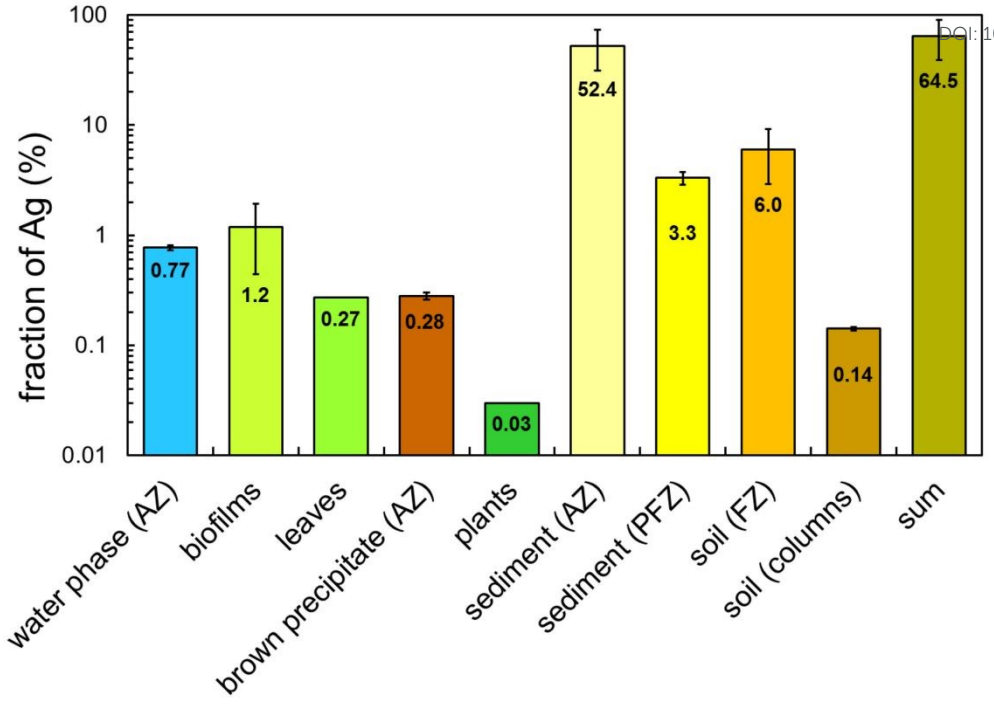

Figure 5. Amount of Ag retained in the compartments assessed in the present study (mass balance). Columns and error bars correspond to mean values and standard deviations determined from 2-11 sampling locations and three replicate samples, respectively. The values above 1% were rounded to one digit after the decimal sign.

3.6 Ecotoxicological impact of Ag-NPs

The feeding activity of gammarids, which was used as sensitive ecotoxicological response variable, was inconsistently affected over time (Figure 6) – a pattern, which was independent of the location of gammarids. The significant reduction in feeding activity before the first Ag-NP pulse (week 11) was unexpected and suggests that the conditions in the mesocosm have not been favorable during the early phases of the experiment. This negative effect disappeared during most subsequent assessments when performed during periods between Ag-NP pulses (Figure 6, A). These data suggest that the concentrations of Ag that have been detected in the water phase (Figure 2) are too low to induce negative effects in gammarids. This is unexpected as

the levels of dissolved Ag approach 5 µg L^{-1} towards the end of the experiment, a concentration exceeding the Ag 72h-LC50 for *G. fossarum*.[64] It may, hence, be concluded that the dissolved complexes formed between Ag^{+} ions and NOM as suggested above, are not biologically available.

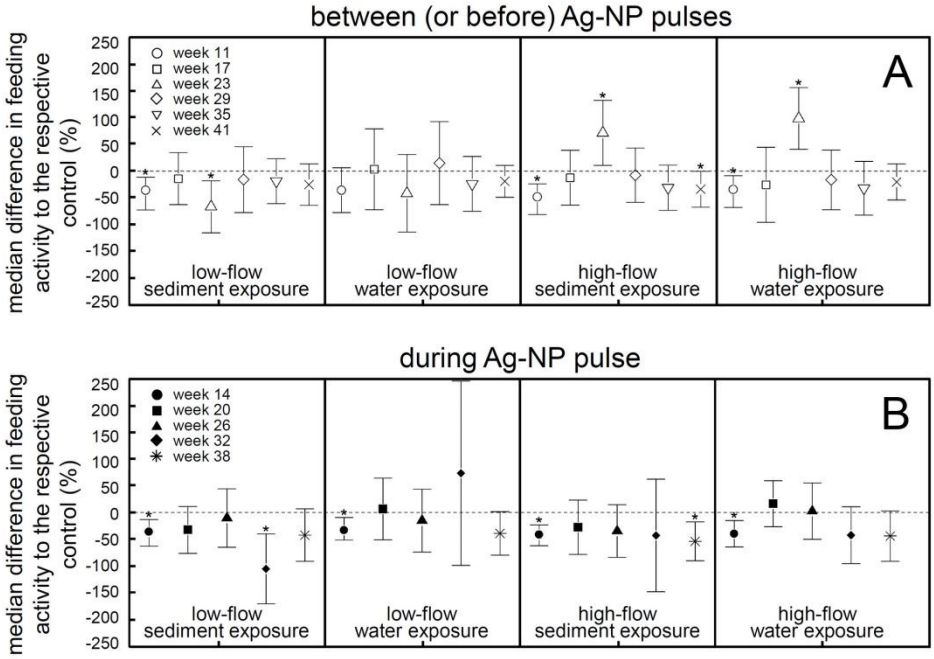

Figure 6. Median difference in the feeding activity of *G. fossarum* expressed relative to the nanoparticle free respective control (dashed line) for exposure phases between (A) and during (B) Ag-NP pulses. The value determined for week 11 represents the exposure period within the control phase (before Ag-NP pulse). Negative values indicate a decreased feeding activity compared to the control. Error bars show the confidence interval (95%). Asterisks (*) denote statistically significant difference to the control (dashed line).

Those *G. fossarum* that have been exposed for seven days in the mesocosm to the Ag-NP pulse show more frequently a reduction in their feeding rate (Figure 6, B) relative to their peers deployed in the mesocosm during periods outside of the pulsed

Ag-NP exposure. Each of the respective scenario (exposure before, during, or between Ag-NP pulses, water or sediment exposure, high or low flow exposure) was compared to a parallel setup where control animals were kept (using same cages) in a stainless steel channel filled with uncontaminated river water. Nonetheless, the effects are inconsistent in magnitude suggesting that the peak Ag-NP concentrations of up to 40 µg L^{-1} were too low to induce a response in the test organisms. Indeed, earlier studies suggest no effects in leaf consumption of *G. fossarum* when exposed to the same Ag-NPs over more than four weeks.[65] Consequently, silver neither in its complexed or nanoparticle form did affect the leaf shredding behavior of invertebrate assessed here, despite concentrations in the mid µg L^{-1} range. Furthermore, the results obtained for amphipods from the sediment exposure scenario indicated that their feeding activity was also not affected negatively by high enrichment of nanoparticles on the sediment surface. The results are in line with our hypothesis 2 which suggests that the biological effects of Ag-NPs on amphipods in aquatic-terrestrial transition zone are controlled by complexation of released ions and low aqueous concentrations of nanoparticles induced by their aquatic aging.

4 Conclusions and environmental implications

In this study, we evaluated the long-term (up to 9 months) fate and effects of citrate-coated Ag-NPs in an aquatic-terrestrial transition zone. Our mesocosm combining thermodynamically and kinetically controlled processes simulates a river bed with flowing river water and a periodically flooded adjacent terrestrial compartment in one system allowing to assess long-term aging, distribution, transport, and effects of ENPs under such conditions.

View Article Online
DOI: 10.1039/D1EN00093D

Despite the high extent of aggregation of Ag-NPs and their immobilization on the sediment surface, a small fraction remains in the water phase for several weeks, which indicates a potential to be transported over large distances in rivers. This fact may represent a potential risk for organisms further downstream of nanoparticle (point) sources. Furthermore, if physico-chemical conditions are changed in river systems for instance during flooding, sedimented Ag-NPs may be remobilized inducing a further downstream transport. Whether or not these remobilized Ag-NPs represent a risk depends on the dynamics of the remobilization and the time frame of the accumulation. More importantly, Ag-NPs can also be transported to terrestrial ecosystems with potential risks over the long-term. Due to the formation of nanoparticle aggregates, we expect only low or negligible vertical migration of nanoparticles into deeper soil and sediment layers. However, we cannot exclude an accelerated propagation of nanoparticles into deeper layers by a turnover of the river bed or due to the formation of preferential flow paths. Due to the extremely slow transport, a significant contamination of ground water resources is only possible on a long-term scale (e.g. several years or even decades) if any at all.

The *G. fossarum* feeding assays suggest that under current field exposure scenarios, where the expected concentrations of Ag-NPs are even lower, effects are unlikely. However, the interplay between aggregation, sedimentation, and attachment on algae and biofilms can lead to the formations of hot spots of immobilized Ag-NPs on the sediment surface. These hot spots can serve as a continuous source of toxic Ag^+ ions leading to enhanced risk for organisms. However, the bioavailability of dissolved Ag^+-NOM complexes formed especially in aquatic systems with high concentrations of organic carbon can significantly control the risk for the biota. Furthermore, the high enrichment of Ag-NPs on algae and leaves can lead to increased risk for the

organisms feeding on these resources and also for the transfer of nanoparticles within the food web. These questions need more attention in future research.

Author information

Corresponding author

*E-mail: metreveli@uni-landau.de

Author contribution

George Metreveli: Conceptualization, methodology, investigation, validation, supervision, project administration, writing - original draft, writing - review & editing.

Sandra Kurtz: Methodology, investigation, writing - original draft, writing - review & editing.

Ricki R. Rosenfeldt: Investigation, writing - review & editing.

Frank Seitz: Investigation, writing - review & editing.

Samuel K. Kumahor: Investigation.

Alexandra Grün: Investigation.

Sondra Klitzke: Writing - review & editing.

Hans-Jörg Vogel: Supervision, writing - review & editing.

Mirco Bundschuh: Supervision, writing - review & editing.

Thomas Baumann: Supervision, Writing - review & editing.

Ralf Schulz: Supervision, writing - review & editing.

Werner Manz: Supervision, writing - review & editing.

Friederike Lang: Supervision, writing - review & editing.

Gabriele E. Schaumann: Conceptualization, supervision, project administration, writing - review & editing.

Conflicts of interest

There are no conflicts to declare.

Acknowledgments

The authors thank the German Research Foundation (DFG) for financial support within research unit INTERNANO ("Mobility, aging and functioning of engineered inorganic nanoparticles at the aquatic-terrestrial interface", FOR 1536, subprojects: SCHA849/16, SCHU2271/5, MA3273/3, KA1139/18, KL2909/1, LA1398/9, BA1592/6, and VO566/12). We are also grateful to Bärbel Schmidt, Roland Vogt, Kilian Kenngott, Zacharias Steinmetz, and Sebastian Scheu for the support in lab and for the supervision of mesocosm experiment. We also thank Dr. Wolfgang Fey for the ICP-MS and ICP-OES measurements and Dr. Dorothee Killmann (University of Koblenz-Landau, Institute of Integrated Science, Department of Biology) for the identification of organisms in biofilm samples.

References

1 D. V. Malmon, T. Dunne and S. L. Reneau, Predicting the fate of sediment and pollutants in river floodplains, *Environ. Sci. Technol.*, 2002, **36**, 2026–2032.

2 M. Bundschuh, J. Filser, S. Lüderwald, M. S. McKee, G. Metreveli, G. E. Schaumann, R. Schulz and S. Wagner, Nanoparticles in the environment: Where do we come from, where do we go to?, *Environ. Sci. Eur.*, 2018, **30**, 6.

3 J. R. Lead, G. E. Batley, P. J. J. Alvarez, M. N. Croteau, R. D. Handy, M. J. McLaughlin, J. D. Judy and K. Schirmer, Nanomaterials in the environment:

Behavior, fate, bioavailability, and effects - An updated review, *Environ. Toxicol. Chem.*, 2018, **37**, 2029–2063.

4 B. P. Colman, C. L. Arnaout, S. Anciaux, C. K. Gunsch, M. F. Hochella, B. Kim, G. V. Lowry, B. M. McGill, B. C. Reinsch, C. J. Richardson, J. M. Unrine, J. P. Wright, L. Y. Yin and E. S. Bernhardt, Low concentrations of silver nanoparticles in biosolids cause adverse ecosystem responses under realistic field scenario, *PLoS One*, 2013, 8, e57189.

5 G. E. Schaumann, A. Philippe, M. Bundschuh, G. Metreveli, S. Klitzke, D. Rakcheev, A. Grün, S. Kumahor, M. Kühn, T. Baumann, F. Lang, W. Manz, R. Schulz and H.-J. Vogel, Understanding the fate and biological effects of Ag- and TiO_2-nanoparticles in the environment: The quest for advanced analytics and interdisciplinary concepts, *Sci. Total Environ.*, 2015, **535**, 3–19.

6 A. Bour, F. Mouchet, J. Silvestre, L. Gauthier and E. Pinelli, Environmentally relevant approaches to assess nanoparticles ecotoxicity: A review, *J. Hazard. Mater.*, 2015, **283**, 764–777.

7 J. I. Kwak and Y.-J. An, The current state of the art in research on engineered nanomaterials and terrestrial environments: Different-scale approaches, *Environ. Res.*, 2016, **151**, 368–382.

8 A. Baun, P. Sayre, K. G. Steinhauser and J. Rose, Regulatory relevant and reliable methods and data for determining the environmental fate of manufactured nanomaterials, *NanoImpact*, 2017, **8**, 1–10.

9 M. Baalousha, G. Cornelis, T. A. J. Kuhlbusch, I. Lynch, C. Nickel, W. Peijnenburg and N. W. van den Brink, Modeling nanomaterial fate and uptake in

the environment: Current knowledge and future trends, *Environ. Sci.: Nano*, 2016, **3**, 323–345.

10 Z. Y. Wang, L. Zhang, J. Zhao and B. S. Xing, Environmental processes and toxicity of metallic nanoparticles in aquatic systems as affected by natural organic matter, *Environ. Sci.: Nano*, 2016, **3**, 240–255.

11 M. Auffan, A. Masion, C. Mouneyrac, C. de Garidel-Thoron, C. O. Hendren, A. Thiery, C. Santaella, L. Giamberini, J.-Y. Bottero, M. R. Wiesner and J. Rose, Contribution of mesocosm testing to a single-step and exposure-driven environmental risk assessment of engineered nanomaterials, *NanoImpact*, 2019, **13**, 66–69.

12 R. Hjorth, L. M. Skjolding, S. N. Sorensen and A. Baun, Regulatory adequacy of aquatic ecotoxicity testing of nanomaterials, *NanoImpact*, 2017, **8**, 28–37.

13 E. Fernández-Pascual, S. Zaman, M. Bork, F. Lang and J. Lange, Long-term mesocosm experiments to investigate degradation of fluorescent tracers, *J. Hydrol.: X*, 2019, **2**, 100014.

14 G. V. Lowry, B. P. Espinasse, A. R. Badireddy, C. J. Richardson, B. C. Reinsch, L. D. Bryant, A. J. Bone, A. Deonarine, S. Chae, M. Therezien, B. P. Colman, H. Hsu-Kim, E. S. Bernhardt, C. W. Matson and M. R. Wiesner, Long-term transformation and fate of manufactured Ag nanoparticles in a simulated large scale freshwater emergent wetland, *Environ. Sci. Technol.*, 2012, **46**, 7027–7036.

15 B. P. Colman, B. Espinasse, C. J. Richardson, C. W. Matson, G. V. Lowry, D. E. Hunt, M. R. Wiesner and E. S. Bernhardt, Emerging contaminant or an old toxin

in disguise? Silver nanoparticle impacts on ecosystems, *Environ. Sci. Technol.*, 2014, **48**, 5229–5236.

16 J. P. Stegemeier, A. Avellan and G. V. Lowry, Effect of initial speciation of copper- and silver-based nanoparticles on their long-term fate and phytoavailability in freshwater wetland mesocosms, *Environ. Sci. Technol.*, 2017, **51**, 12114–12122.

17 Y. H. El-Farhan, N. M. DeNovio, J. S. Herman and G. M. Hornberger, Mobilization and transport of soil particles during infiltration experiments in an agricultural field, Shenandoah Valley, Virginia, *Environ. Sci. Technol.*, 2000, **34**, 3555–3559.

18 B. E. Vencalek, S. N. Laughton, E. Spielman-Sun, S. M. Rodrigues, J. M. Unrine, G. V. Lowry and K. B. Gregory, In situ measurement of CuO and $Cu(OH)_2$ nanoparticle dissolution rates in quiescent freshwater mesocosms, *Environ. Sci. Technol. Lett.*, 2016, **3**, 375–380.

19 A. J. Bone, C. W. Matson, B. P. Colman, X. Y. Yang, J. N. Meyer and R. T. Di Giulio, Silver nanoparticle toxicity to Atlantic killifish (*Fundulus heteroclitus*) and *Caenorhabditis elegans*: A comparison of mesocosm, microcosm, and conventional laboratory studies, *Environ. Toxicol. Chem.*, 2015, **34**, 275–282.

20 M. K. Yeo and D. H. Nam, Influence of different types of nanomaterials on their bioaccumulation in a paddy microcosm: A comparison of TiO_2 nanoparticles and nanotubes, *Environ. Pollut.*, 2013, **178**, 166–172.

21 P. E. Buffet, M. Richard, F. Caupos, A. Vergnoux, H. Perrein-Ettajani, A. Luna-Acosta, F. Akcha, J. C. Amiard, C. Amiard-Triquet, M. Guibbolini, C. Risso-De Faverney, H. Thomas-Guyon, P. Reip, A. Dybowska, D. Berhanu, E. Valsami-

Jones and C. Mouneyrac, A mesocosm study of fate and effects of CuO nanoparticles on endobenthic species (*Scrobicularia plana*, *Hediste diversicolor*), *Environ. Sci. Technol.*, 2013, **47**, 1620–1628.

22 P. E. Buffet, A. Zalouk-Vergnoux, A. Chatel, B. Berthet, I. Metais, H. Perrein-Ettajani, L. Poirier, A. Luna-Acosta, H. Thomas-Guyon, C. Risso-de Faverney, M. Guibbolini, D. Gilliland, E. Valsami-Jones and C. Mouneyrac, A marine mesocosm study on the environmental fate of silver nanoparticles and toxicity effects on two endobenthic species: The ragworm *Hediste diversicolor* and the bivalve mollusc *Scrobicularia plana*, *Sci. Total Environ.*, 2014, **470**, 1151–1159.

23 J. L. Ferry, P. Craig, C. Hexel, P. Sisco, R. Frey, P. L. Pennington, M. H. Fulton, I. G. Scott, A. W. Decho, S. Kashiwada, C. J. Murphy and T. J. Shaw, Transfer of gold nanoparticles from the water column to the estuarine food web, *Nat. Nanotechnol.*, 2009, **4**, 441–444.

24 C. Mouneyrac, P. E. Buffet, L. Poirier, A. Zalouk-Vergnoux, M. Guibbolini, C. Risso-de Faverney, D. Gilliland, D. Berhanu, A. Dybowska, A. Chatel, H. Perrein-Ettajni, J. F. Pan, H. Thomas-Guyon, P. Reip and E. Valsami-Jones, Fate and effects of metal-based nanoparticles in two marine invertebrates, the bivalve mollusc *Scrobicularia plana* and the annelid polychaete *Hediste diversicolor*, *Environ. Sci. Pollut. Res.*, 2014, **21**, 7899–7912.

25 L. F. Baker, R. S. King, J. M. Unrine, B. T. Castellon, G. V. Lowry and C. W. Matson, Press or pulse exposures determine the environmental fate of cerium nanoparticles in stream mesocosms, *Environ. Toxicol. Chem.*, 2016, **35**, 1213–1223.

26 K. J. Kulacki, B. J. Cardinale, A. A. Keller, R. Bier and H. Dickson, How do stream organisms respond to, and influence, the concentration of titanium dioxide

nanoparticles? A mesocosm study with algae and herbivores, *Environ. Toxicol. Chem.*, 2012, **31**, 2414–2422.

27 A. Bour, F. Mouchet, S. Cadarsi, J. Silvestre, L. Verneuil, D. Baque, E. Chauvet, J. M. Bonzom, C. Pagnout, H. Clivot, I. Fourquaux, M. Tella, M. Auffan, L. Gauthier and E. Pinelli, Toxicity of CeO_2 nanoparticles on a freshwater experimental trophic chain: A study in environmentally relevant conditions through the use of mesocosms, *Nanotoxicology*, 2016, **10**, 245–255.

28 M. Tella, M. Auffan, L. Brousset, J. Issartel, I. Kieffer, C. Pailles, E. Morel, C. Santaella, B. Angeletti, E. Artells, J. Rose, A. Thiery and J. Y. Bottero, Transfer, transformation, and impacts of ceria nanomaterials in aquatic mesocosms simulating a pond ecosystem, *Environ. Sci. Technol.*, 2014, **48**, 9004–9013.

29 M. Tella, M. Auffan, L. Brousset, E. Morel, O. Proux, C. Chaneac, B. Angeletti, C. Pailles, E. Artells, C. Santaella, J. Rose, A. Thiery and J. Y. Bottero, Chronic dosing of a simulated pond ecosystem in indoor aquatic mesocosms: Fate and transport of CeO_2 nanoparticles, *Environ. Sci.: Nano*, 2015, **2**, 653–663.

30 A. Ozaki, E. Adams, C. Binh, T. Z. Tong, J. F. Gaillard, K. A. Gray and J. J. Kelly, One-time addition of nano-TiO_2 triggers short-term responses in benthic bacterial communities in artificial streams, *Microb. Ecol.*, 2016, **71**, 266–275.

31 L. M. Furtado, M. E. Hoque, D. F. Mitrano, J. F. Ranville, B. Cheever, P. C. Frost, M. A. Xenopoulos, H. Hintelmann and C. D. Metcalfe, The persistence and transformation of silver nanoparticles in littoral lake mesocosms monitored using various analytical techniques, *Environ. Chem.*, 2014, **11**, 419–430.

32 L. M. Furtado, B. C. Norman, M. A. Xenopoulos, P. C. Frost, C. D. Metcalfe and H. Hintelmann, Environmental fate of silver nanoparticles in boreal lake ecosystems, *Environ. Sci. Technol.*, 2015, **49**, 8441–8450.

33 B. Jovanovic, G. Bezirci, A. S. Cagan, J. Coppens, E. E. Levi, Z. Oluz, E. Tuncel, H. Duran and M. Beklioglu, Food web effects of titanium dioxide nanoparticles in an outdoor freshwater mesocosm experiment, *Nanotoxicology*, 2016, **10**, 902–912.

34 J. M. Burns, P. L. Pennington, P. N. Sisco, R. Frey, S. Kashiwada, M. H. Fulton, G. I. Scott, A. W. Decho, C. J. Murphy, T. J. Shaw and J. L. Ferry, Surface charge controls the fate of Au nanorods in saline estuaries, *Environ. Sci. Technol.*, 2013, **47**, 12844–12851.

35 D. Cleveland, S. E. Long, P. L. Pennington, E. Cooper, M. H. Fulton, G. I. Scott, T. Brewer, J. Davis, E. J. Petersen and L. Wood, Pilot estuarine mesocosm study on the environmental fate of silver nanomaterials leached from consumer products, *Sci. Total Environ.*, 2012, **421**, 267–272.

36 B. Kim, M. Murayama, B. P. Colman and M. F. Hochella, Characterization and environmental implications of nano- and larger TiO_2 particles in sewage sludge, and soils amended with sewage sludge, *J. Environ. Monitor.*, 2012, **14**, 1129–1137.

37 J. D. Moore, J. P. Stegemeier, K. Bibby, S. M. Marinakos, G. V. Lowry and K. B. Gregory, Impacts of pristine and transformed Ag and Cu engineered nanomaterials on surficial sediment microbial communities appear short-lived, *Environ. Sci. Technol.*, 2016, **50**, 2641–2651.

38 A. Schierz, B. Espinasse, M. R. Wiesner, J. H. Bisesi, T. Sabo-Attwood and P. L. Ferguson, Fate of single walled carbon nanotubes in wetland ecosystems, *Environ. Sci.: Nano*, 2014, **1**, 574–583.

39 A. Avellan, M. Simonin, S. M. Anderson, N. K. Geitner, N. Bossa, E. Spielman-Sun, E. S. Bernhardt, B. T. Castellon, B. P. Colman, J. L. Cooper, M. Ho, M. F. Hochella, H. Hsu-Kim, S. Inoue, R. S. King, S. Laughton, C. W. Matson, B. G. Perrotta, C. J. Richardson, J. M. Unrine, M. R. Wiesner and G. V. Lowry, Differential reactivity of copper- and gold-based nanomaterials controls their seasonal biogeochemical cycling and fate in a freshwater wetland mesocosm, *Environ. Sci. Technol.*, 2020, **54**, 1533–1544.

40 M. E. Vance, T. Kuiken, E. P. Vejerano, S. P. McGinnis, M. F. Hochella, D. Rejeski and M. S. Hull, Nanotechnology in the real world: Redeveloping the nanomaterial consumer products inventory, *Beilstein J Nanotech*, 2015, **6**, 1769–1780.

41 L. Maltby, S. A. Clayton, R. M. Wood and N. McLoughlin, Evaluation of the *Gammarus pulex* in situ feeding assay as a biomonitor of water quality: Robustness, responsiveness, and relevance, *Environ. Toxicol. Chem.*, 2002, **21**, 361–368.

42 H. Finnern, W. Grottenthaler, D. Kühn, W. Pälchen, W.-G. Schraps and H. Sponagel, *Bodenkundliche Kartieranleitung*, Bundesanstalt für Geowissenschaften und Rohstoffe, Geologische Landesämter in der Bundesrepublik Deutschland, Hannover, 4th edn., 1994.

43 G. Metreveli, A. Philippe and G. E. Schaumann, Disaggregation of silver nanoparticle homoaggregates in a river water matrix, *Sci. Total Environ.*, 2015, **535**, 35–44.

44 G. Metreveli, B. Frombold, F. Seitz, A. Grün, A. Philippe, R. R. Rosenfeldt, M. Bundschuh, R. Schulz, W. Manz and G. E. Schaumann, Impact of chemical composition of ecotoxicological test media on the stability and aggregation status of silver nanoparticles, *Environ. Sci.: Nano*, 2016, **3**, 418–433.

45 F. Seitz, R. R. Rosenfeldt, S. Schneider, R. Schulz and M. Bundschuh, Size-, surface- and crystalline structure composition-related effects of titanium dioxide nanoparticles during their aquatic life cycle, *Sci. Total Environ.*, 2014, **493**, 891–897.

46 D. G. Altman, D. Machin, T. N. Bryant and M. J. Gardner, *Statistics with confidence: Confidence intervals and statistical guidelines*, BMJ Books, London, 2nd edn., 2000.

47 N. Sepehrnia, O. Fishkis, B. Huwe and J. Bachmann, Natural colloid mobilization and leaching in wettable and water repellent soil under saturated condition, *J. Hydrol. Hydromech.*, 2018, **66**, 271–278.

48 M. Y. Lin, H. M. Lindsay, D. A. Weitz, R. C. Ball, R. Klein and P. Meakin, Universality in colloid aggregation, *Nature*, 1989, **339**, 360–362.

49 S. Maillette, C. Peyrot, T. Purkait, M. Iqbal, J. G. C. Veinot and K. J. Wilkinson, Heteroagglomeration of nanosilver with colloidal SiO_2 and clay, *Environ. Chem.*, 2017, **14**, 1–8.

50 L. Li, M. Stoiber, A. Wimmer, Z. Xu, C. Lindenblatt, B. Helmreich and M. Schuster, To what extent can full-scale wastewater treatment plant effluent influence the occurrence of silver-based nanoparticles in surface waters?, *Environ. Sci. Technol.*, 2016, **50**, 6327–6333.

51 L. Guo and P. H. Santschi, in *Environmental colloids and particles: Behaviour, separation and characterisation*, John Wiley & Sons, Ltd, 2007, vol. 10, pp. 159–221.

52 J. Ren, Z. Li and F.-S. Wong, A new method for the prediction of pore size distribution and MWCO of ultrafiltration membranes, *J. Membr. Sci.*, 2006, **279**, 558–569.

53 Y. Jung, G. E. Schaumann, S. Baik and G. Metreveli, Effects of hydrophobicity-based fractions of Pony Lake fulvic acid on the colloidal stability and dissolution of oppositely charged surface-coated silver nanoparticles, *Environ. Chem.*, 2020, **17**, 400–412.

54 Y. Jung, G. Metreveli, C.-B. Park, S. Baik and G. E. Schaumann, Implications of Pony Lake fulvic acid for the aggregation and dissolution of oppositely charged surface-coated silver nanoparticles and their ecotoxicological effects on *Daphnia magna*, *Environ. Sci. Technol.*, 2018, **52**, 436–445.

55 Z. Chen, P. G. C. Campbell and C. Fortin, Silver binding by humic acid as determined by equilibrium ion-exchange and dialysis, *J. Phys. Chem. A*, 2012, **116**, 6532–6539.

56 W.-C. Hou, B. Stuart, R. Howes and R. G. Zepp, Sunlight-driven reduction of silver ions by natural organic matter: Formation and transformation of silver nanoparticles, *Environ. Sci. Technol.*, 2013, **47**, 7713–7721.

57 N. F. Adegboyega, V. K. Sharma, K. Siskova, R. Zbořil, M. Sohn, B. J. Schultz and S. Banerjee, Interactions of aqueous Ag^+ with fulvic acids: Mechanisms of silver nanoparticle formation and investigation of stability, *Environ. Sci. Technol.*, 2013, **47**, 757–764.

58 L. Degenkolb, G. Metreveli, A. Philippe, A. Brandt, K. Leopold, L. Zehlike, H.-J. Vogel, G. E. Schaumann, T. Baumann, M. Kaupenjohann, F. Lang, S. Kumahor and S. Klitzke, Retention and remobilization mechanisms of environmentally aged silver nanoparticles in an artificial riverbank filtration system, *Sci. Total Environ.*, 2018, **645**, 192–204.

59 R. J. Stevenson and P. C. Esselman, in *River conservation: Challenges and opportunities*, Fundacion BBVA, 2013, pp. 77–104.

60 P. Das, C. D. Metcalfe and M. A. Xenopoulos, Interactive effects of silver nanoparticles and phosphorus on phytoplankton growth in natural waters, *Environ. Sci. Technol.*, 2014, **48**, 4573–4580.

61 Y. Yue, X. Li, L. Sigg, M. J.-F. Suter, S. Pillai, R. Behra and K. Schirmer, Interaction of silver nanoparticles with algae and fish cells: A side by side comparison, *Journal of Nanobiotechnology*, 2017, **15**, 16.

62 K. W. Cummins, Structure and function of stream ecosystems, *BioScience*, 1974, **24**, 631–641.

63 M. Bundschuh, D. Englert, R. R. Rosenfeldt, R. Bundschuh, A. Feckler, S. Lüderwald, F. Seitz, J. P. Zubrod and R. Schulz, Nanoparticles transported from aquatic to terrestrial ecosystems via emerging aquatic insects compromise subsidy quality, *Sci. Rep.*, 2019, **9**, 15676.

64 K. Mehennaoui, A. Georgantzopoulou, V. Felten, J. Andreï, M. Garaud, S. Cambier, T. Serchi, S. Pain-Devin, F. Guérold, J.-N. Audinot, L. Giambérini and A. C. Gutleb, *Gammarus fossarum* (Crustacea, Amphipoda) as a model organism to study the effects of silver nanoparticles, *Sci. Total Environ.*, 2016, **566–567**, 1649–1659.

65 S. Lüderwald, T. Schell, K. Newton, R. Salau, F. Seitz, R. R. Rosenfeldt, V. Dackermann, G. Metreveli, R. Schulz and M. Bundschuh, Exposure pathway dependent effects of titanium dioxide and silver nanoparticles on the benthic amphipod *Gammarus fossarum*, *Aquat. Toxicol.*, 2019, **212**, 47–53.